Supporting Information

Eggshell membrane-derived metal sulfide catalysts for seawater splitting

Lingyu Cui,[1,2] Lan Zhang[2,4,5*],Yi Shen[1,2,3*]

[1]School of Food Science and Engineering, South China University of Technology, Guangzhou 510640, China

[2]China-Singapore International Joint Research Institute, Guangzhou Knowledge City, Guangzhou 510663, China

[3]Overseas Expertise Introduction Center for Discipline Innovation of Food Nutrition and Human Health (111 Center), Guangzhou, 510641, China

[4]School of Mechanical and Aerospace Engineering, Nanyang Technological University, Singapore 639798, Singapore

[5]Energy Research Institute at NTU (ERI@N), Nanyang Technological University, 1 CleanTech Loop, Singapore 637141, Singapore

[*]Corresponding authors Emails: zhanglan@ntu.edu.sg (L. Z) and feyshen@scut.edu.cn (Y. S.)

Table S1
Composition of feedstock and pyrolysis temperature for sample syntheses.

Samples		Chemicals				Hydrothermal temperature /℃	Calcination temperature /℃
		$Co(NO_3)_2·6H_2O$ /mmol	$Fe(NO_3)_3·9H_2O$ /mmol	$Ni(NO_3)_2·6H_2O$ /mmol	ESM /g		
Co_9S_8/ESM-T	Co_9S_8/ESM-200	0.9	-	-	0.4	200	-
	Co_9S_8/ESM-800						800
	Co_9S_8/ESM-900						900
	Co_9S_8/ESM-1000						1000
Co_8FeS_8/ESM-T	Co_8FeS_8/ESM-200	0.8	0.1	-	0.4	200	-
	Co_8FeS_8/ESM-800						800
	Co_8FeS_8/ESM-900						900
	Co_8FeS_8/ESM-1000						1000
FeS_x/ESM-T	FeS_x/ESM-200	-	0.9	-	0.4	200	-
	FeS_x/ESM-800						800
	FeS_x/ESM-900						900
	FeS_x/ESM-1000						1000
Ni_9S_8/ESM-T	Ni_9S_8/ESM-900	-	-	0.9	0.4	200	900
Ni_8FeS_8/ESM-T	Ni_9S_8/ESM-900	-	0.1	0.8	0.4	200	900

Table S2
Comparison of the OER performance of the Co-based electrocatalysts.

Electrocatalyst	Overpotential (mV) (j=10 mA cm^{-2})	Tafel slope (mV dec^{-1})	Electrolyte	Substrate	Loading (μg cm^{-2})	Reference
Co_8FeS_8/ESM-900	270	51.04	1 M KOH	GCE	120	This work
CoPS	280.7	87	1 M KOH	NF	769	R1
NiCoSe|S/BP	285	116	1 M KOH	GCE	160	R2
Fe-Co-Ni-S_x/NF	280	86	1 M KOH	NF	-	R3
N/O-dual doped carbon coated CoNPs (EK-b)	378	60	1 M KOH	CC	205	R4
Co_4Ni_1S/CC	296	52	1 M KOH	CC	520	R5
CoS/MoS_2	281	79	1 M KOH	GCE	132	R6
FeCoNiP@P-rGO	354	155	1 M KOH	-	-	R7
Co@S-MoO_x NSs	274	62	1 M KOH	NF	-	R8
Co-Ni-S	368	86	1 M KOH	CC	1000	R9
Co@$CoMoO_x$-α-CrOOH	278	67.9	1 M KOH	NF	-	R10
CNO@NSG	287.4	66.3	1 M KOH	NF	100	R11
Ni-Co/Ni-Co-O-P@CS	310	151	1 M KOH	-	-	R12
P, S-Co_xO_y/Cu@CuS NWs	280	73.9	1 M KOH	CF	184	R13

Fig. S1 Digital photos of eggshell membranes.

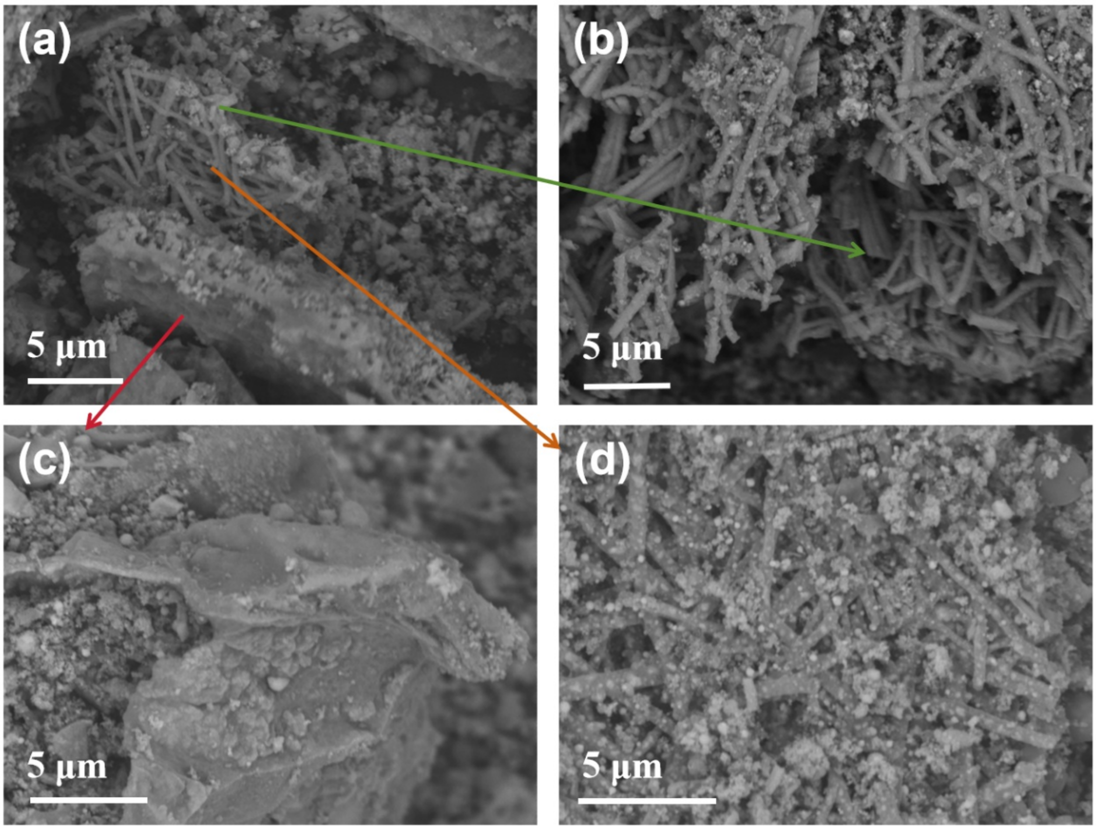

Fig. S2 FESEM images of (a) individual ESM fragments, (b) the inner shell membrane, (c) the limiting shell membrane, and (d) the outer membrane after carbonization.

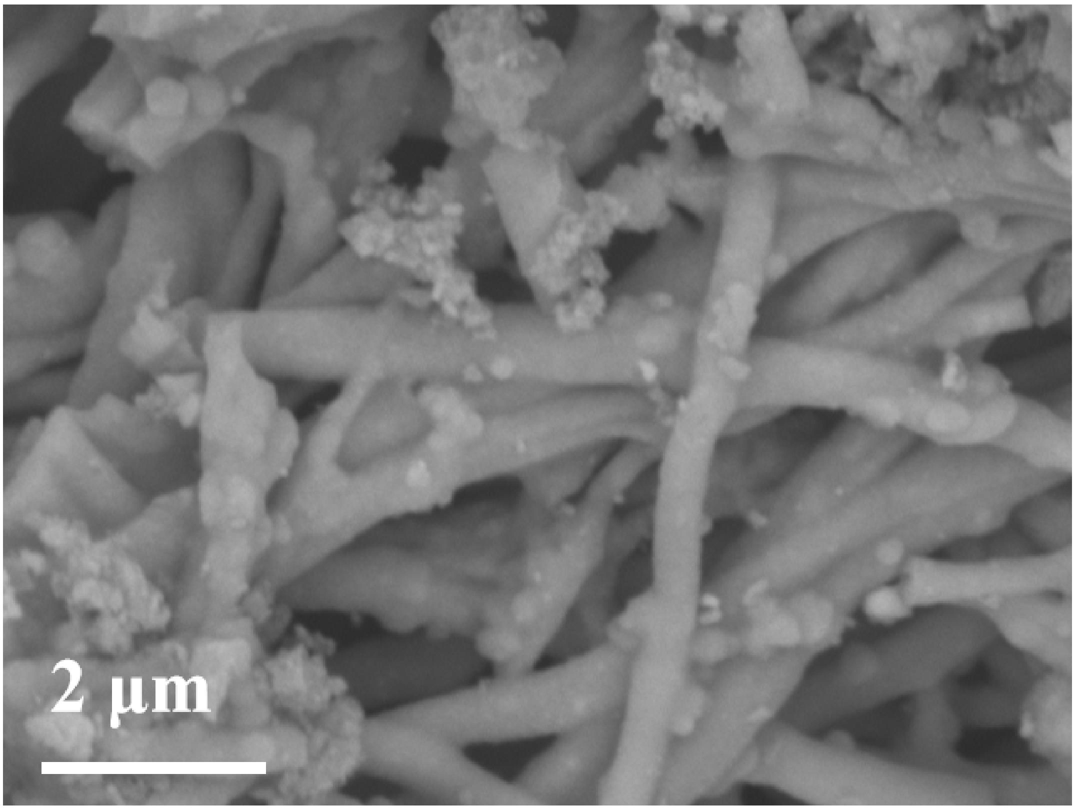

Fig. S3 FESEM image of Co_9S_8/ESM-900.

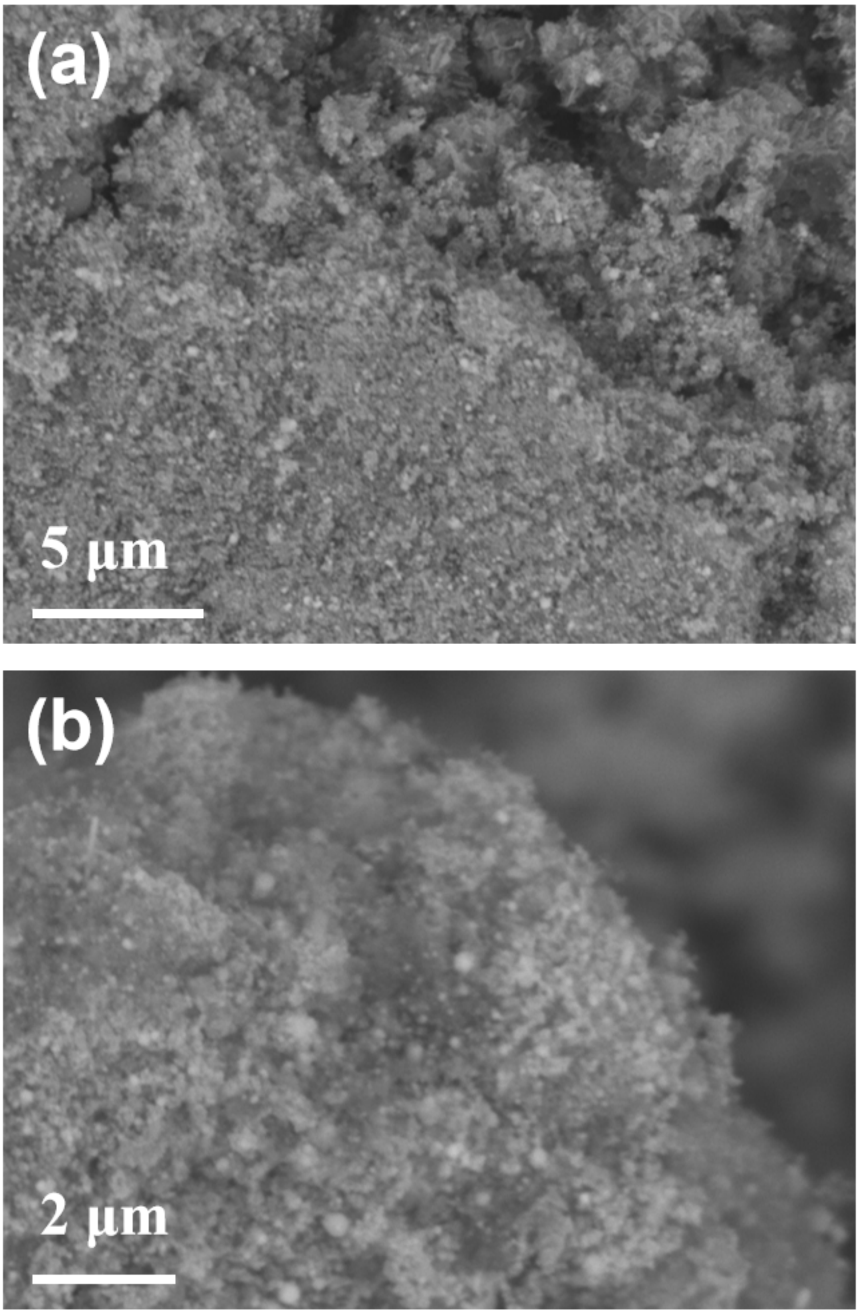

Fig. S4 SEM images of FeS_x/ESM-900.

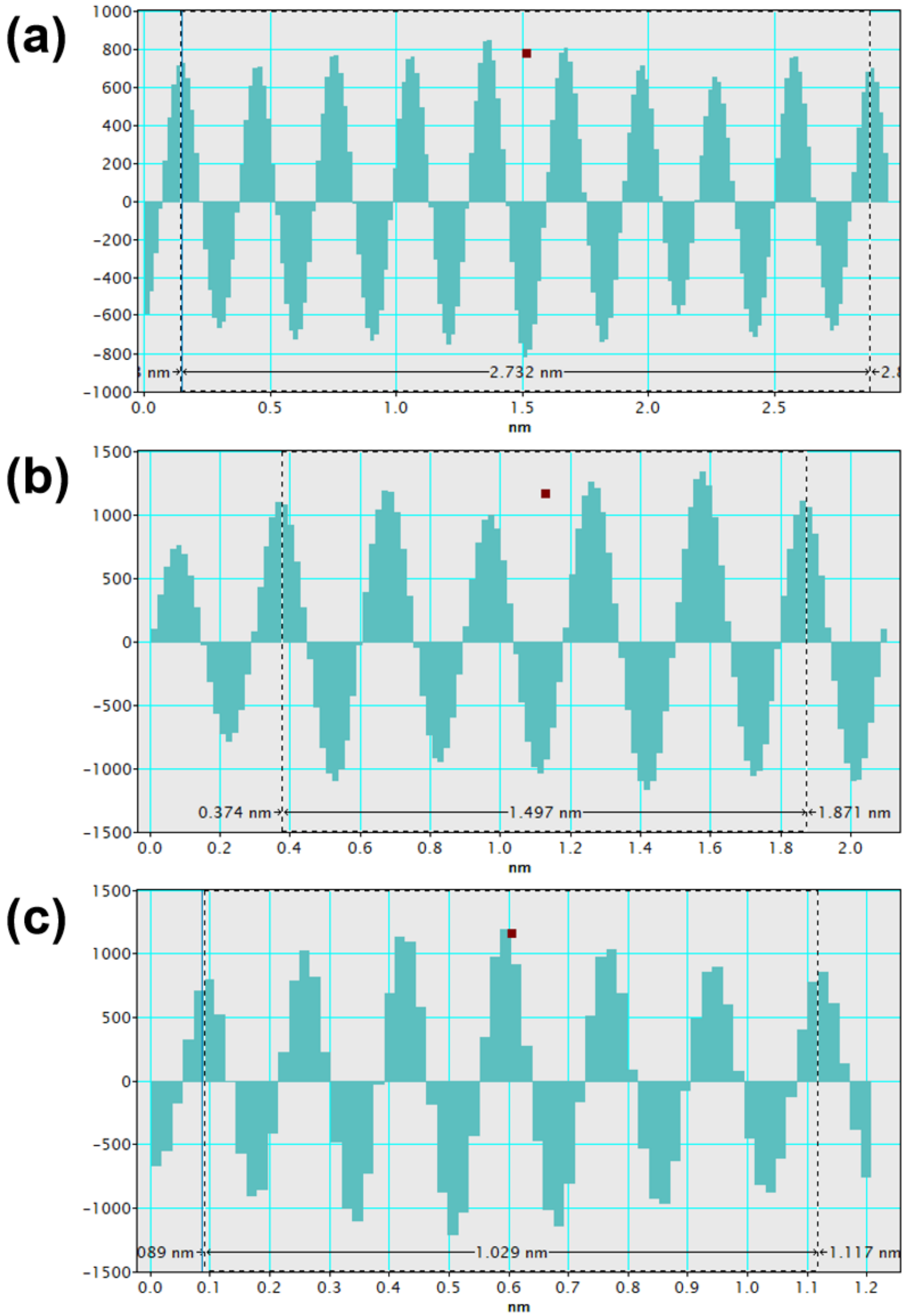

Fig. S5 Intensity profiles within (a) region 1 and (b-c) region 2 shown in Fig. 1.

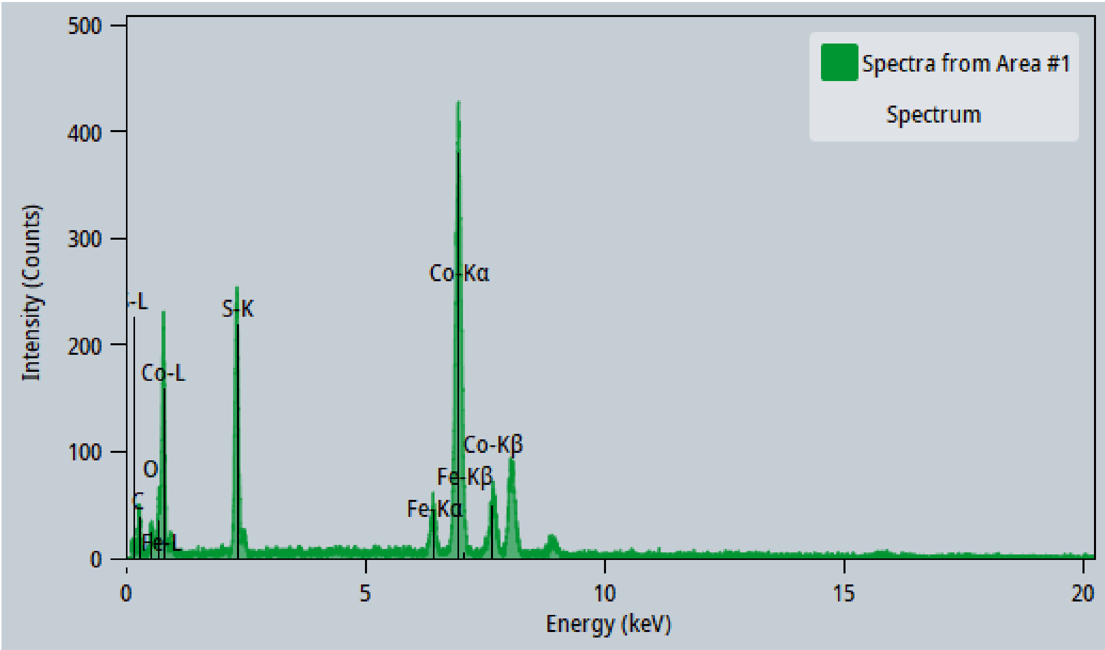

Fig. S6 EDS spectrum of Co_8FeS_8/ESM-900.

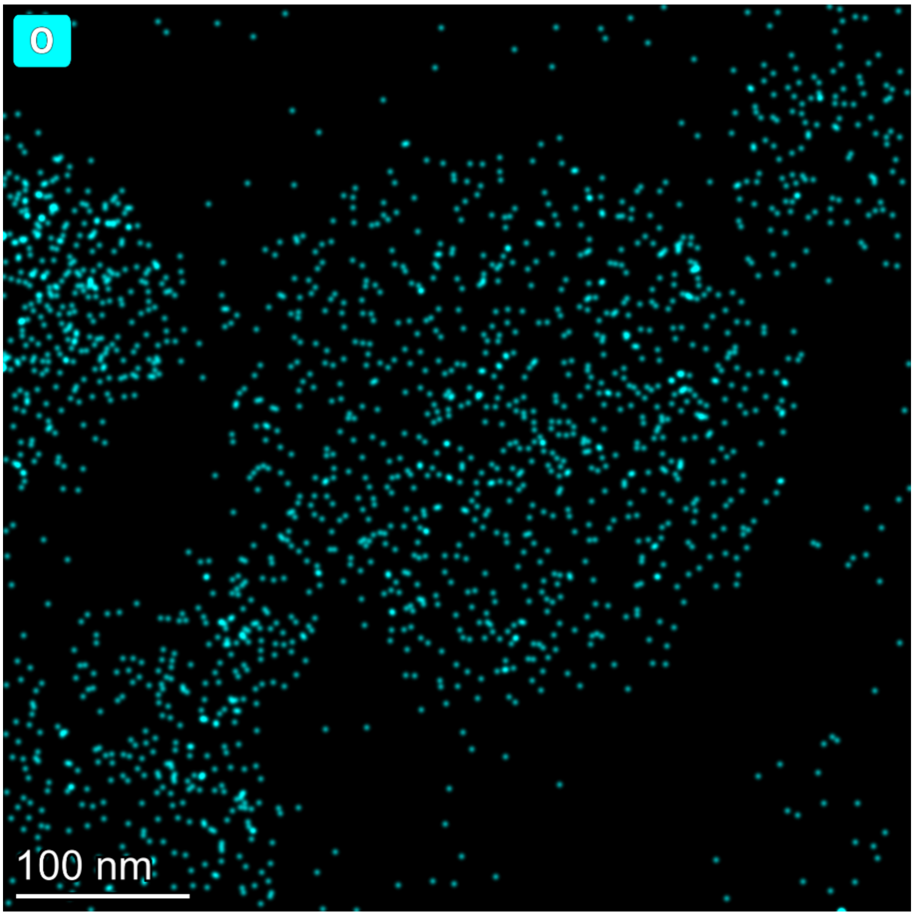

Fig. S7 EDS element mappings of oxygen.

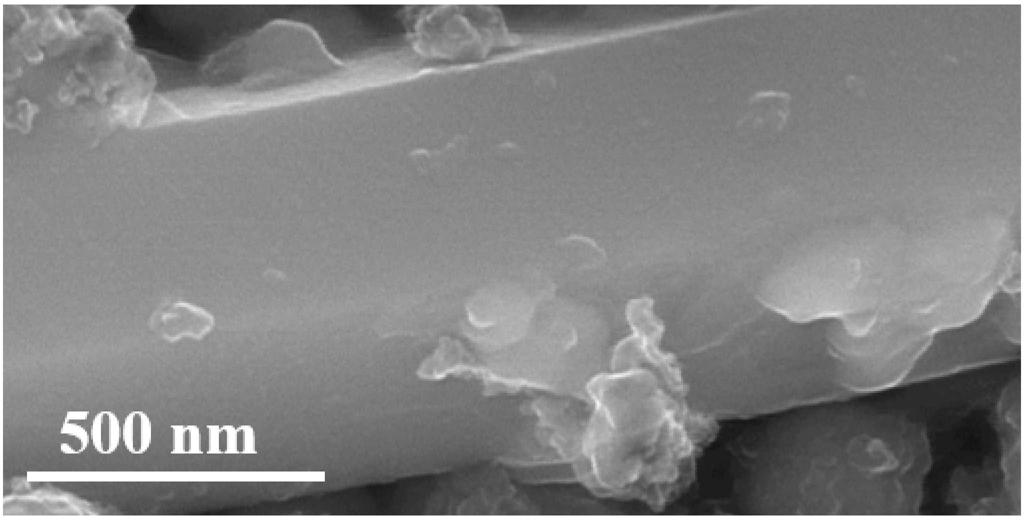

Fig. S8 SEM images of the support.

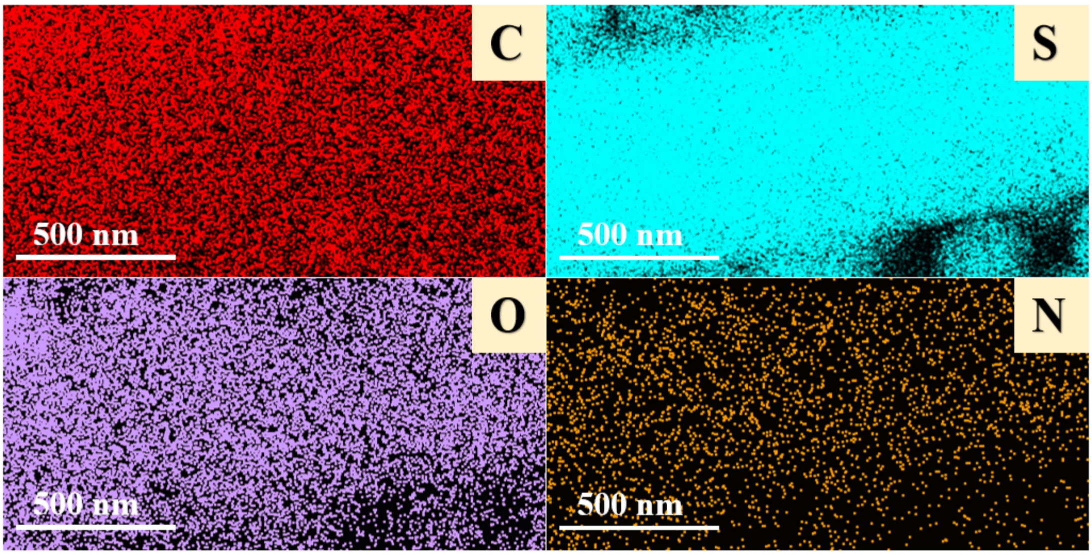

Fig. S9 EDS element mapping images of the support.

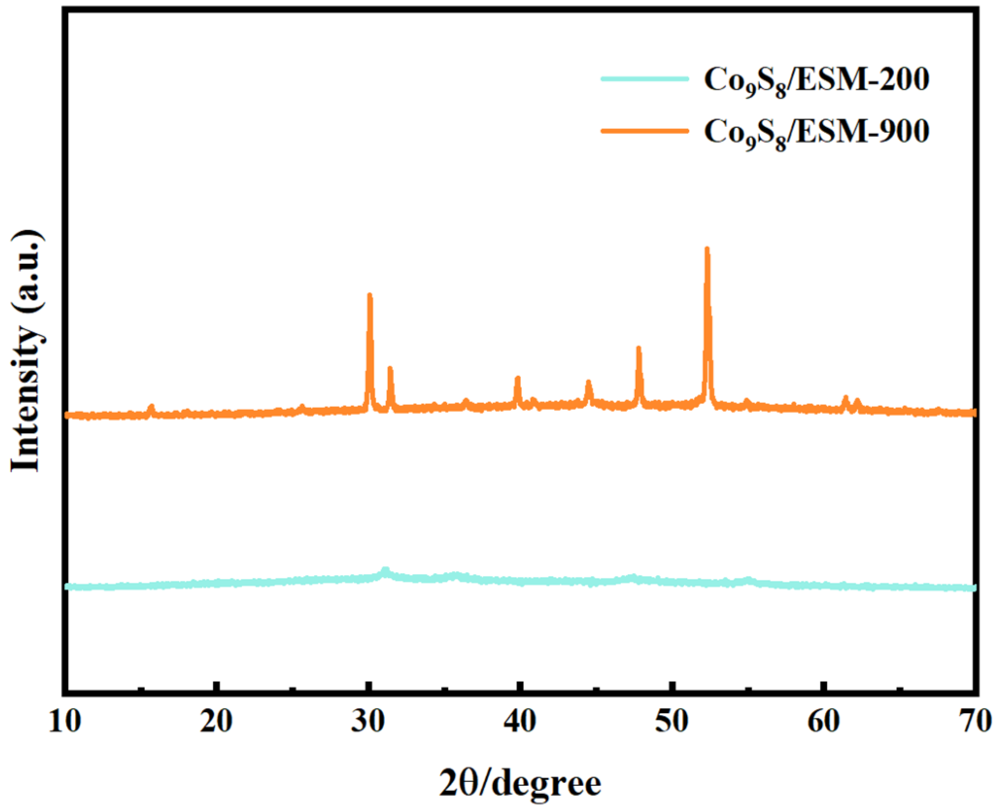

Fig. S10 XRD patterns of Co_9S_8/ESM-200 and Co_9S_8/ESM-900.

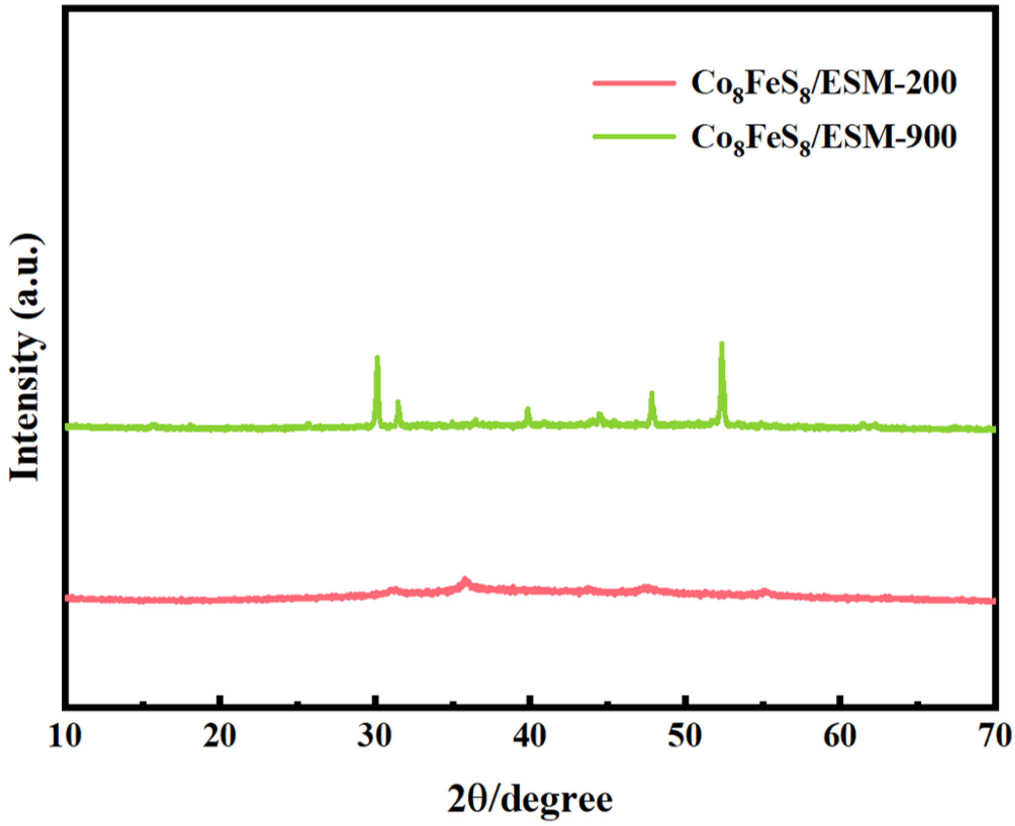

Fig. S11 XRD patterns of Co_8FeS_8/ESM-200 and Co_8FeS_8/ESM-900.

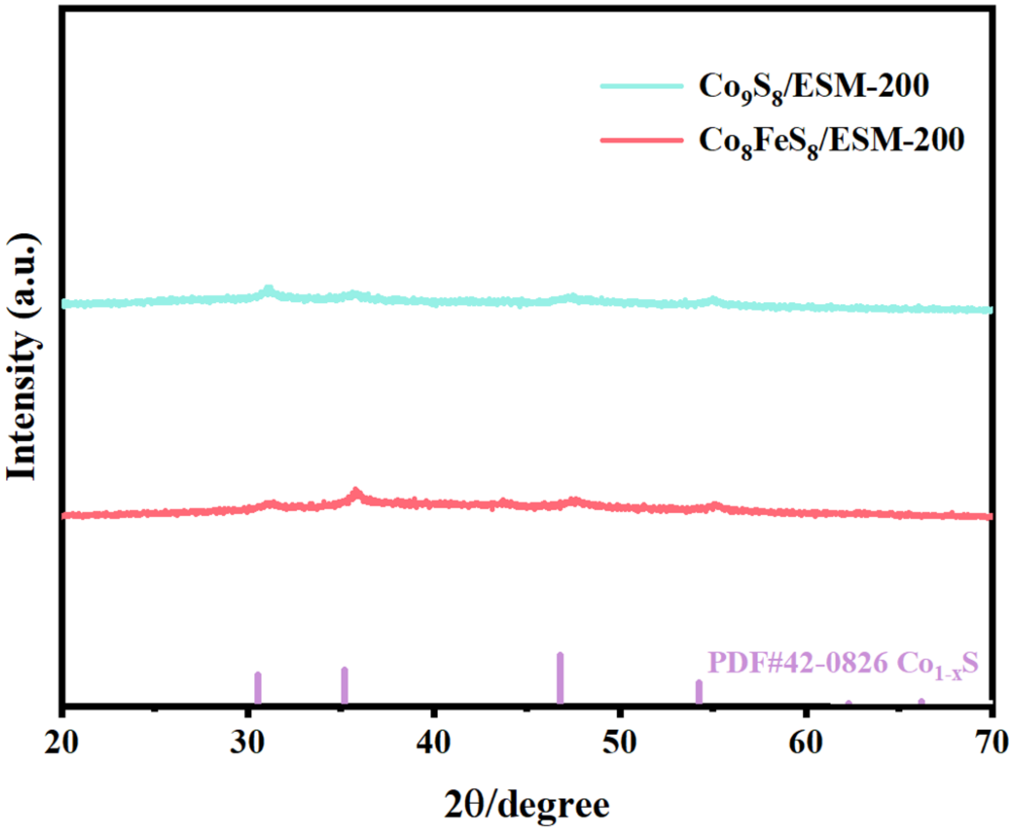

Fig. S12 XRD patterns of Co_9S_8/ESM-200 and Co_8FeS_8/ESM-200.

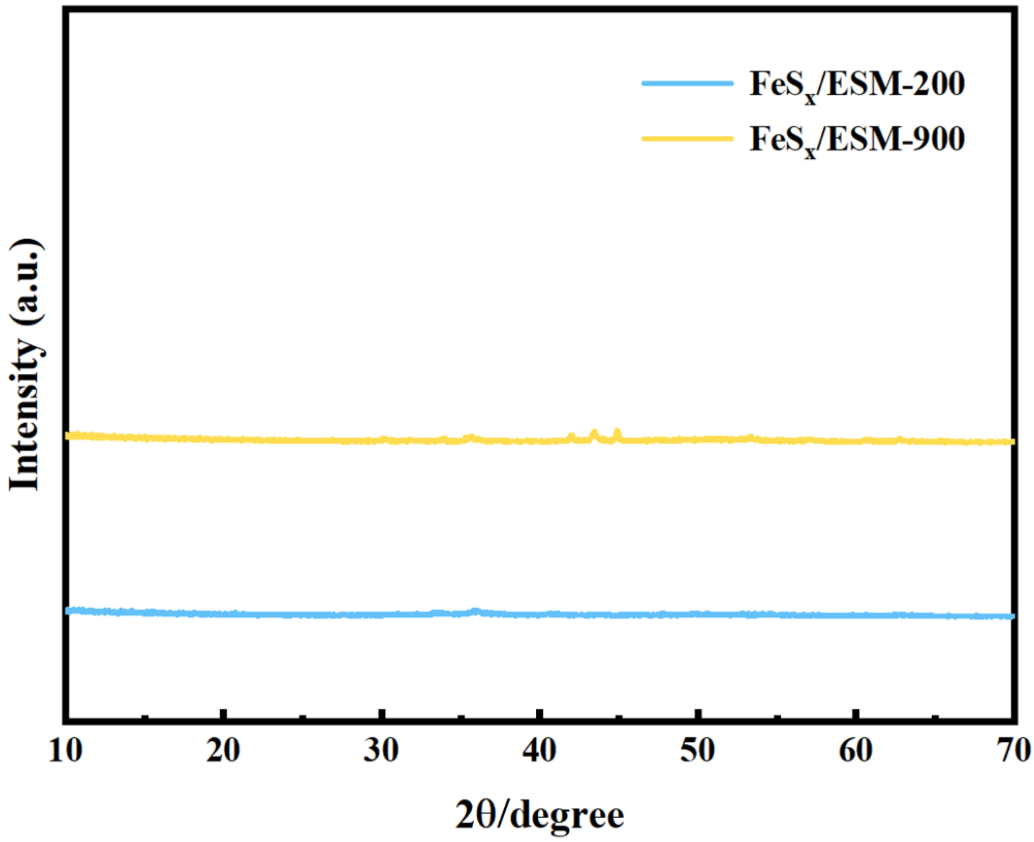

Fig. S13 XRD patterns of FeS_x/ESM-200 and FeS_x/ESM-900.

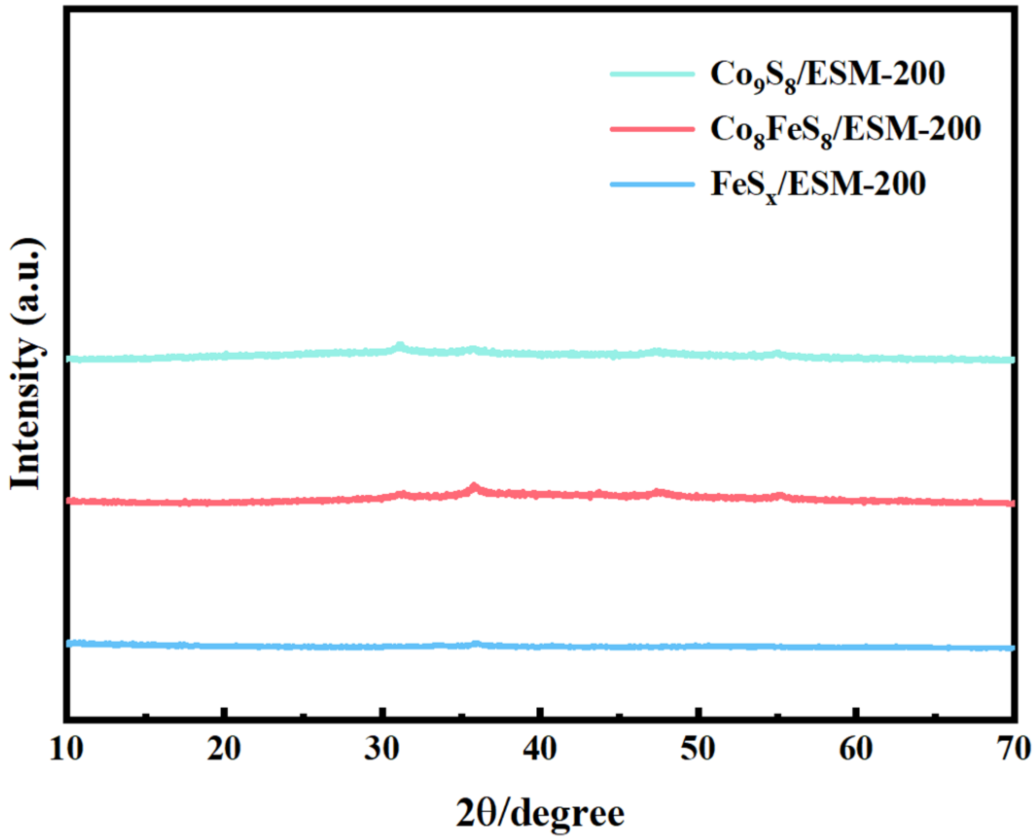

Fig. S14 XRD patterns of Co_9S_8/ESM-200, Co_8FeS_8/ESM-200 and FeS_x/ESM-200.

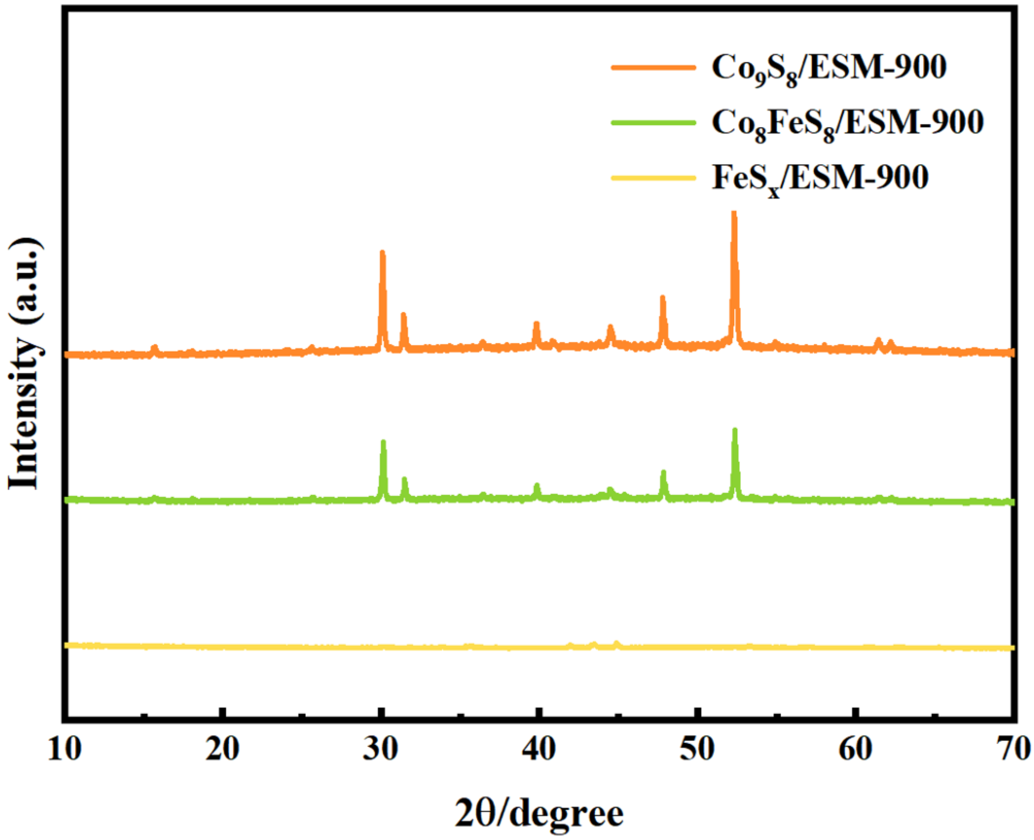

Fig. S15 XRD patterns of Co_9S_8/ESM-900, Co_8FeS_8/ESM-900 and FeS_x/ESM-900.

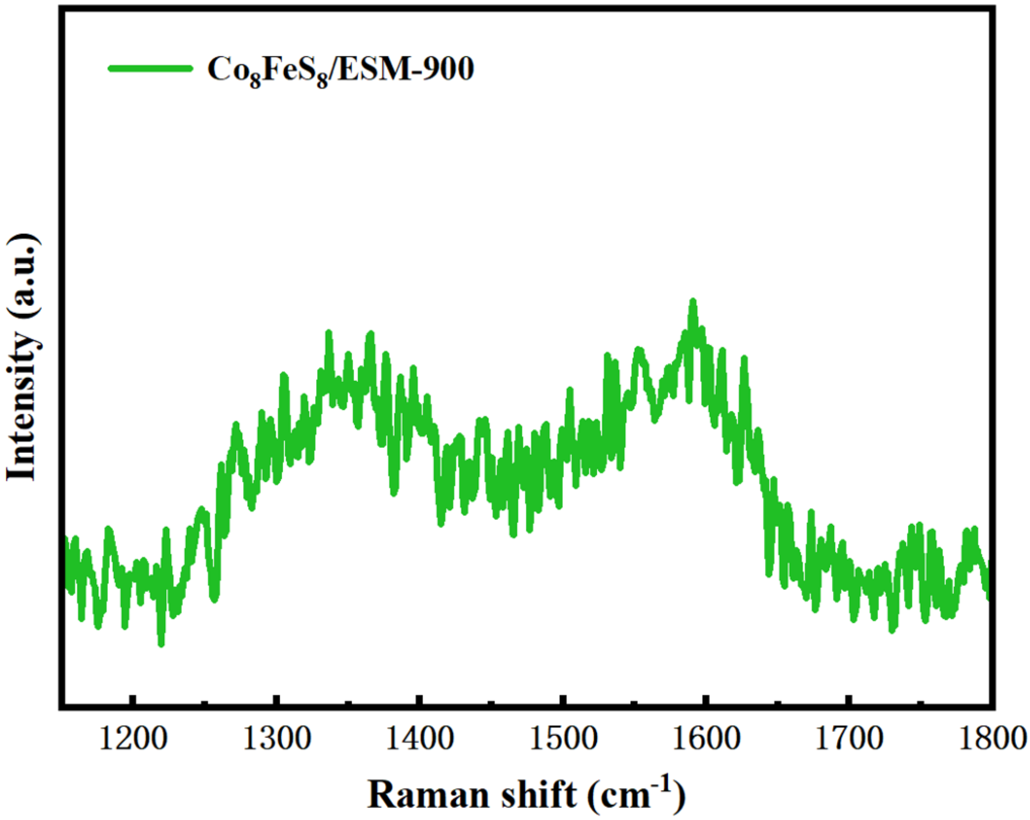

Fig. S16 Raman spectrum of Co_8FeS_8/ESM-900.

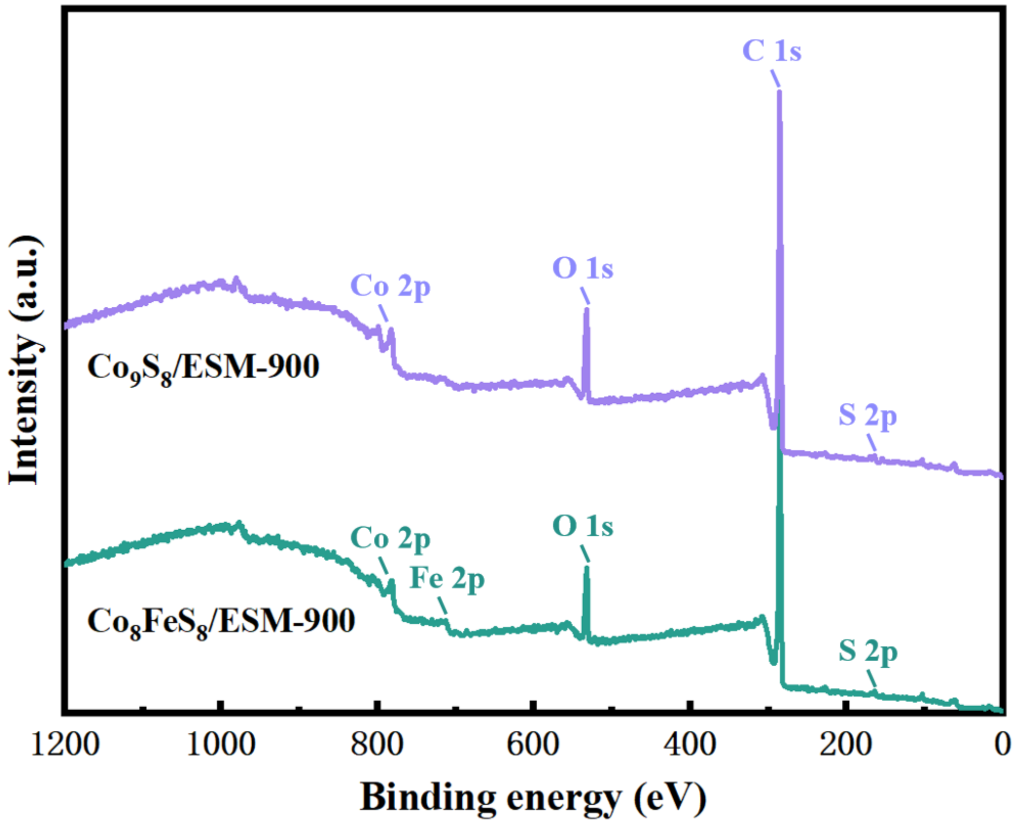

Fig. S17 Surveys spectra of Co_9S_8/ESM-900 and Co_8FeS_8/ESM-900.

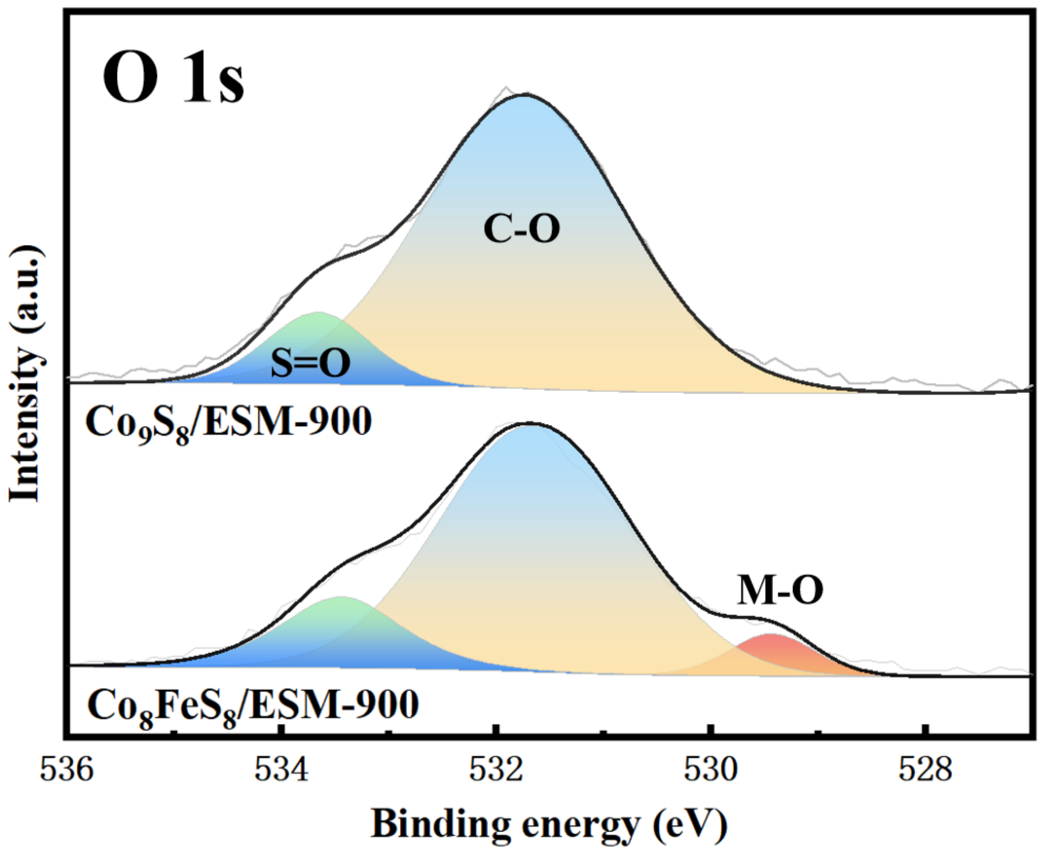

Fig. S18 XPS spectra of O1s.

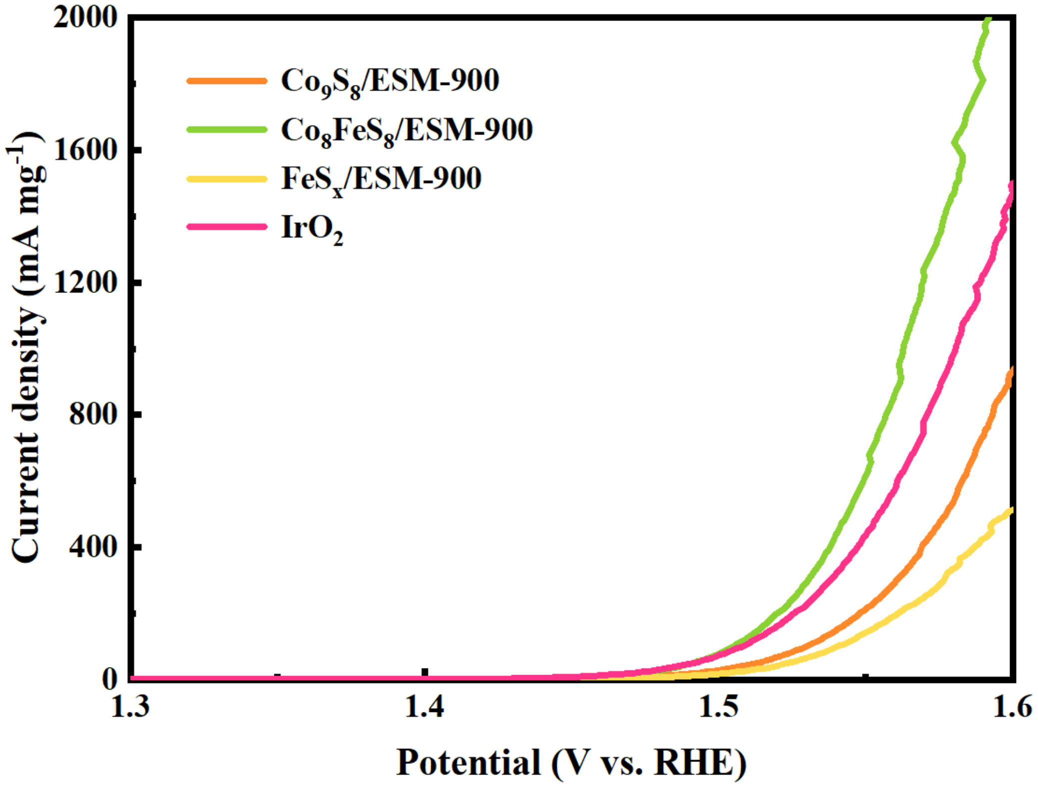

Fig. S19 Mass-normalized LSV curves of Co_9S_8/ESM-900, Co_8FeS_8/ESM-900, FeS_x/ESM-900 and IrO_2 recorded in 1 M KOH.

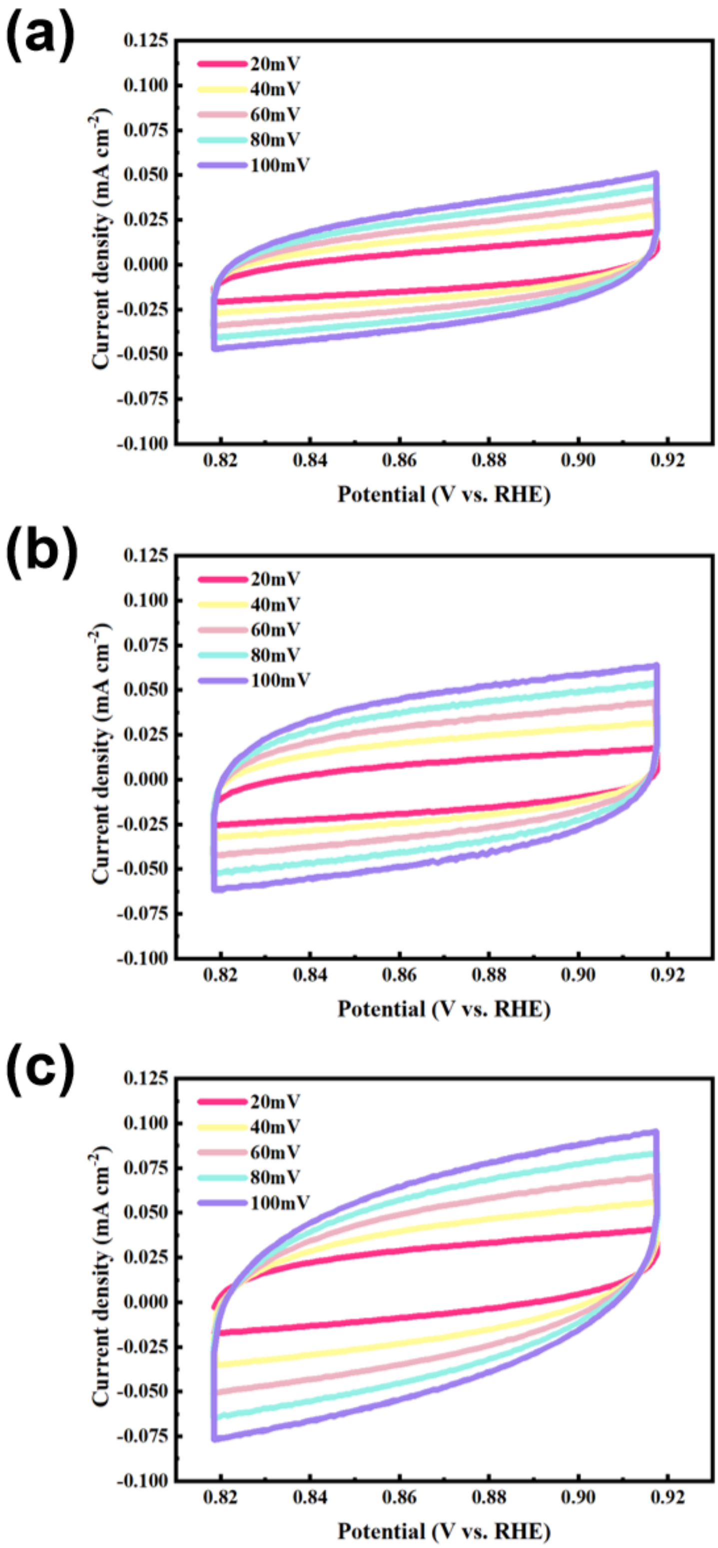

Fig. S20 CVs of (a) Co_9S_8/ESM-900, (b) Co_8FeS_8/ESM-900, and (c) FeS_x/ESM-900 recorded with varying scan rates.

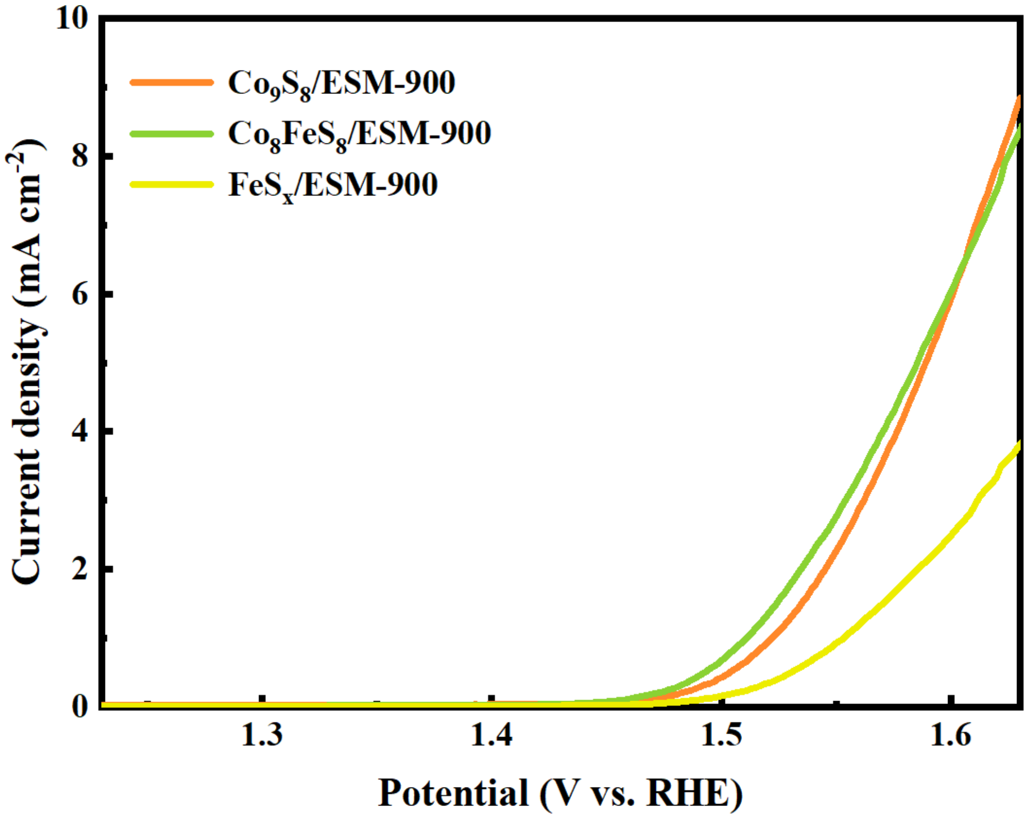

Fig. S21 ECSA-normalized LSV curves of Co_9S_8/ESM-900, Co_8FeS_8/ESM-900 and FeS_x/ESM-900 recorded in 1 M KOH.

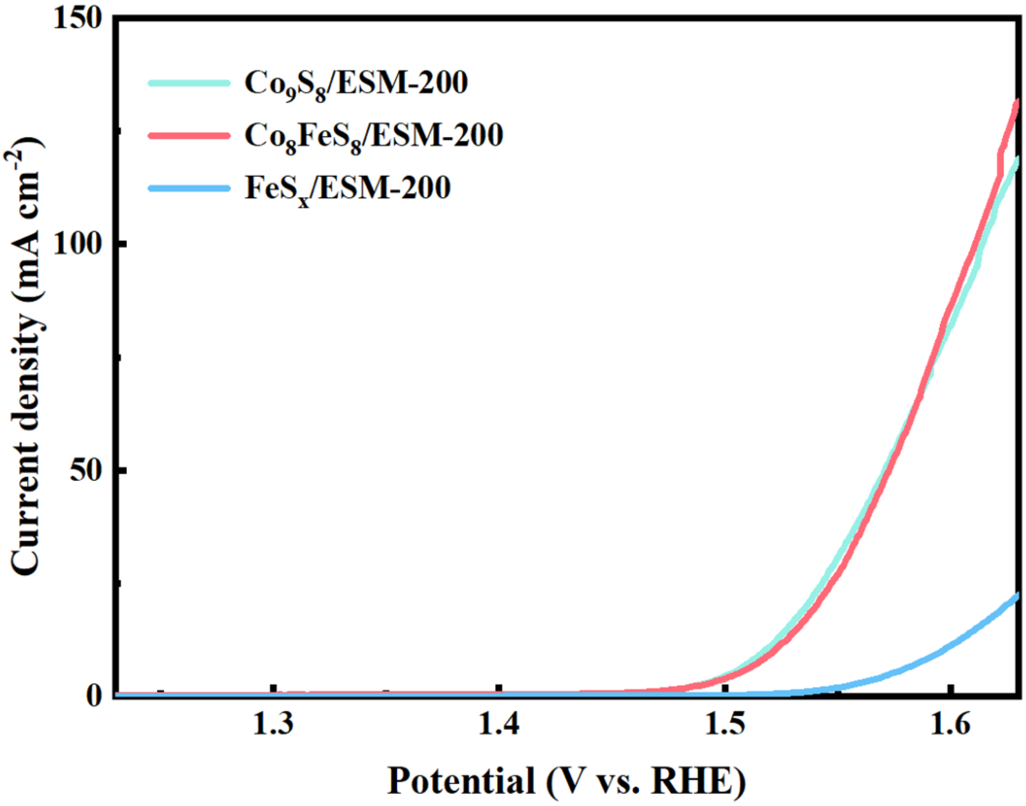

Fig. S22 LSV curves of Co_9S_8/ESM-200, Co_8FeS_8/ESM-200 and FeS_x/ESM-200 recorded in 1 M KOH.

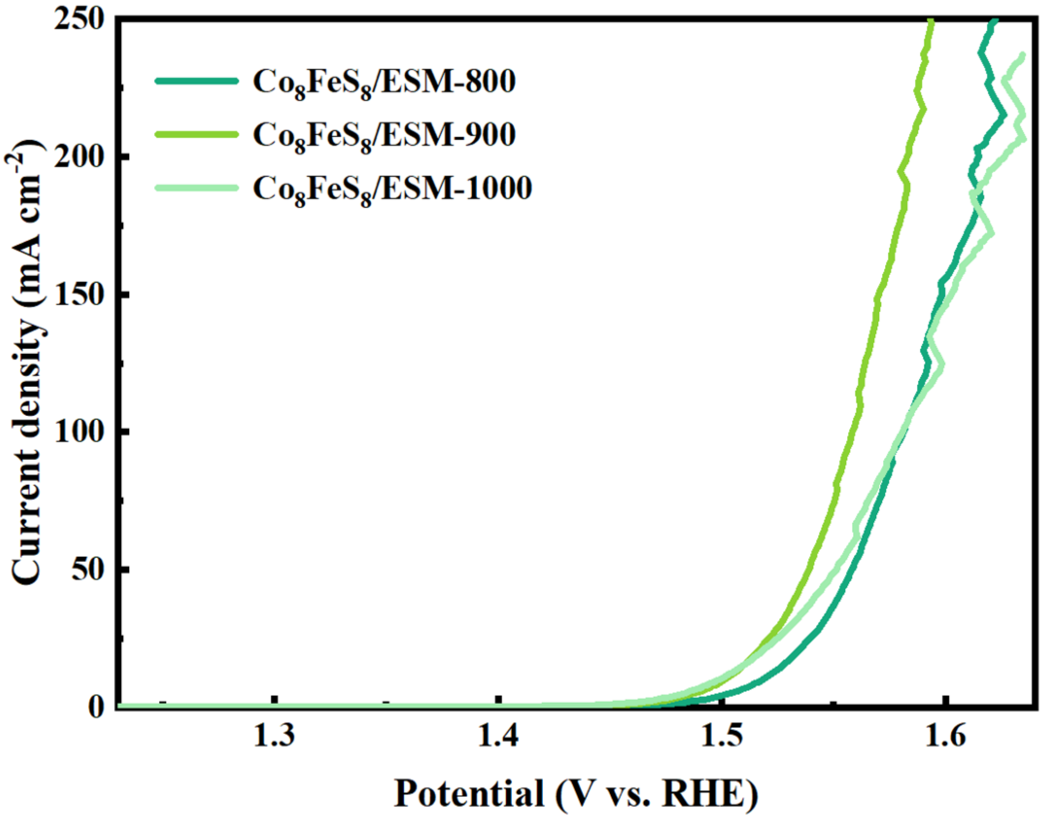

Fig. S23 LSV curves of Co_8FeS_8/ESM-800, Co_8FeS_8/ESM-900 and Co_8FeS_8/ESM-1000 recorded in 1 M KOH.

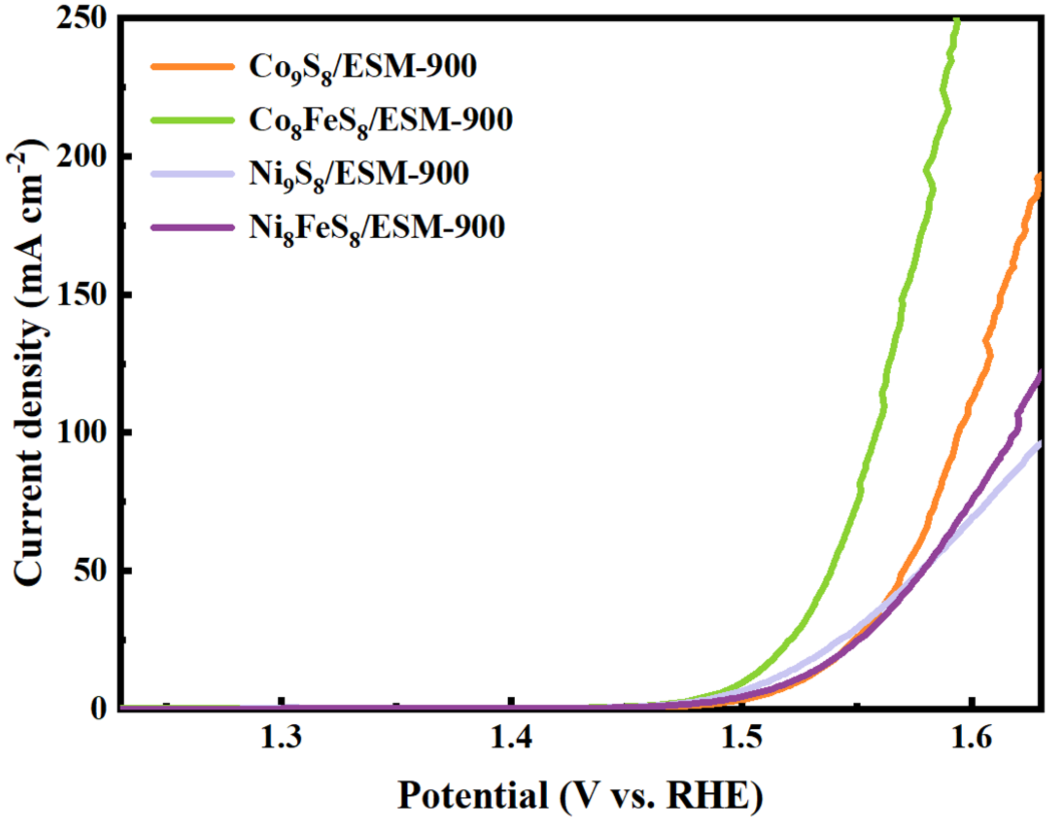

Fig. S24 LSV curves of Co_9S_8/ESM-900, Co_8FeS_8/ESM-900, Ni_9S_8/ESM-900 and Ni_8FeS_8/ESM-900 recorded in 1 M KOH.

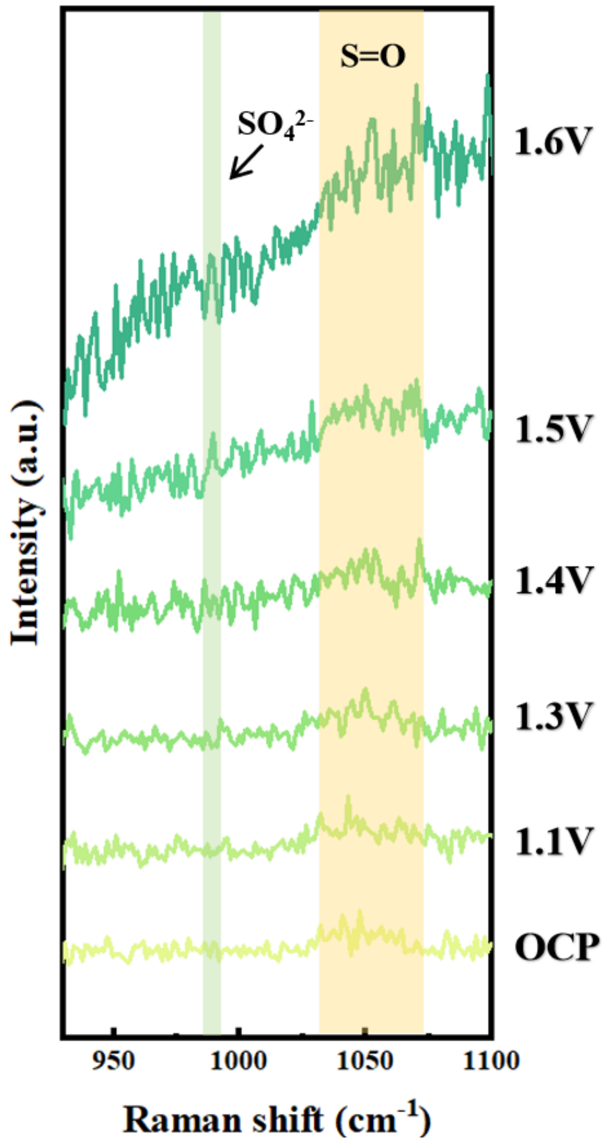

Fig. S25 In situ Raman spectroscopy of Co_8FeS_8/ESM-900.

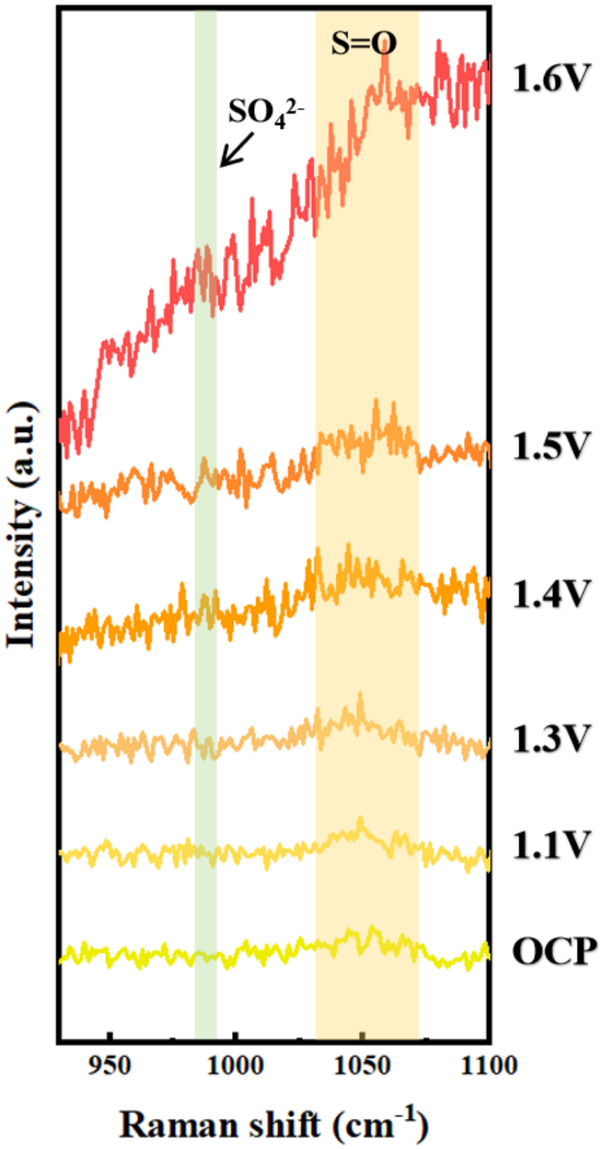

Fig. S26 In situ Raman spectroscopy of Co_9S_8/ESM-900.

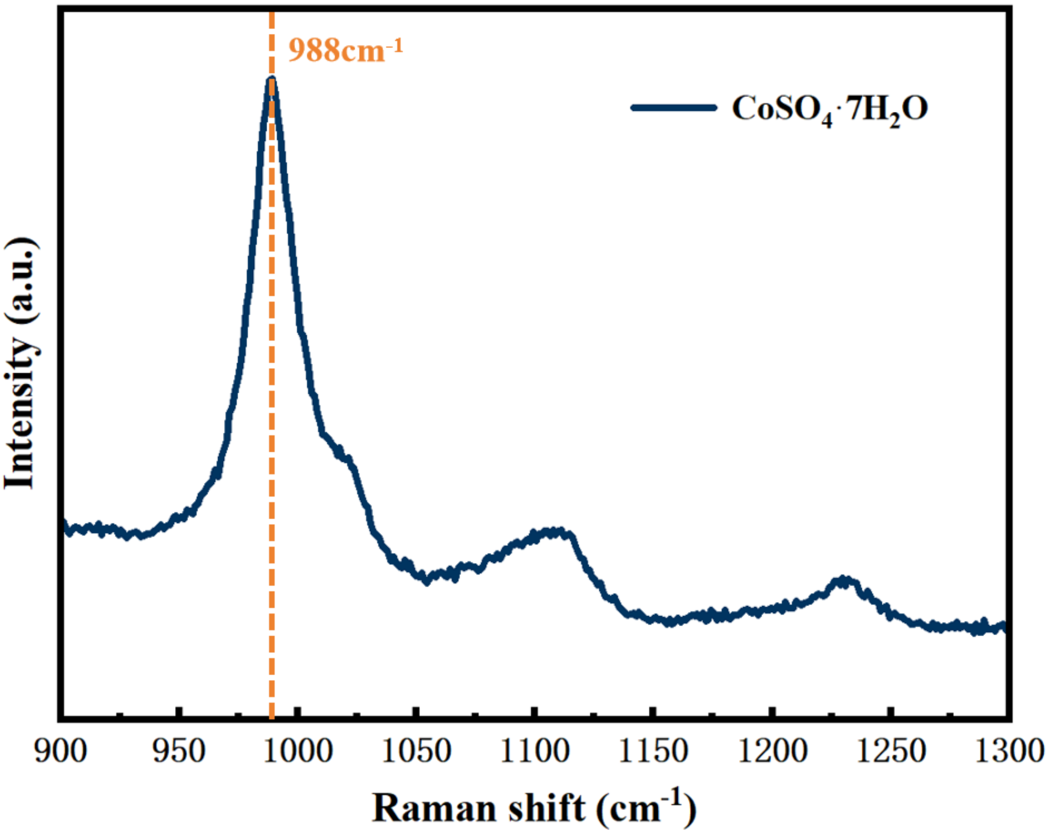

Fig. S27 Raman spectroscopy of $CoSO_4·7H_2O$.

Fig. S28 Schematic diagram of the apparatus for the Faraday efficiency test.

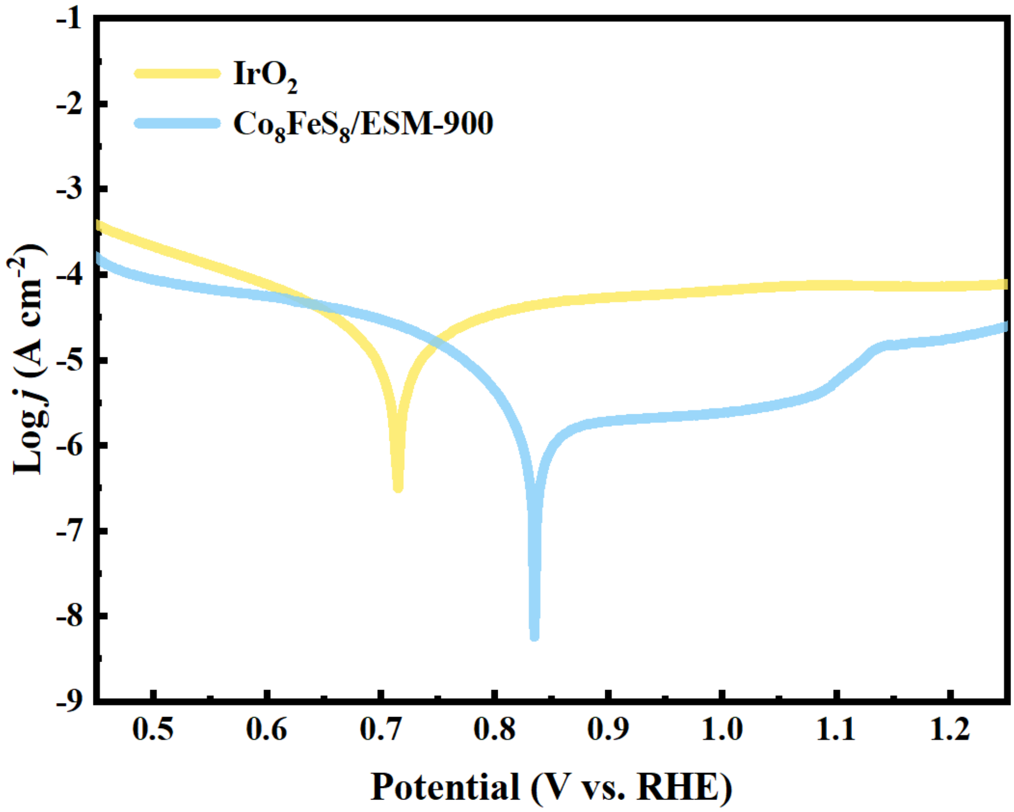

Fig. S29 Corrosion polarization curves of Co_8FeS_8/ESM-900 and IrO_2 in 1 M KOH + seawater.

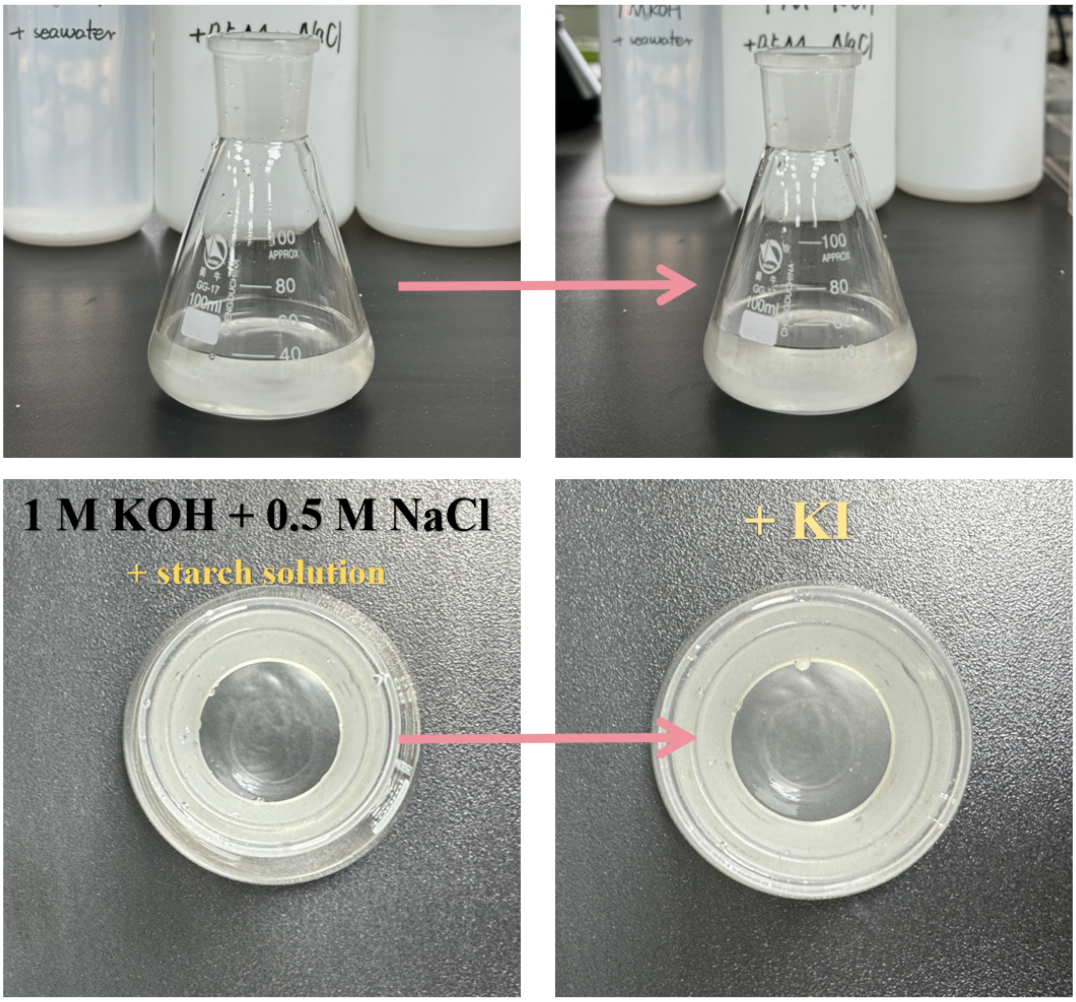

Fig. S30 Digital photos of illustrating the determination of ClO^- in simulated seawater.

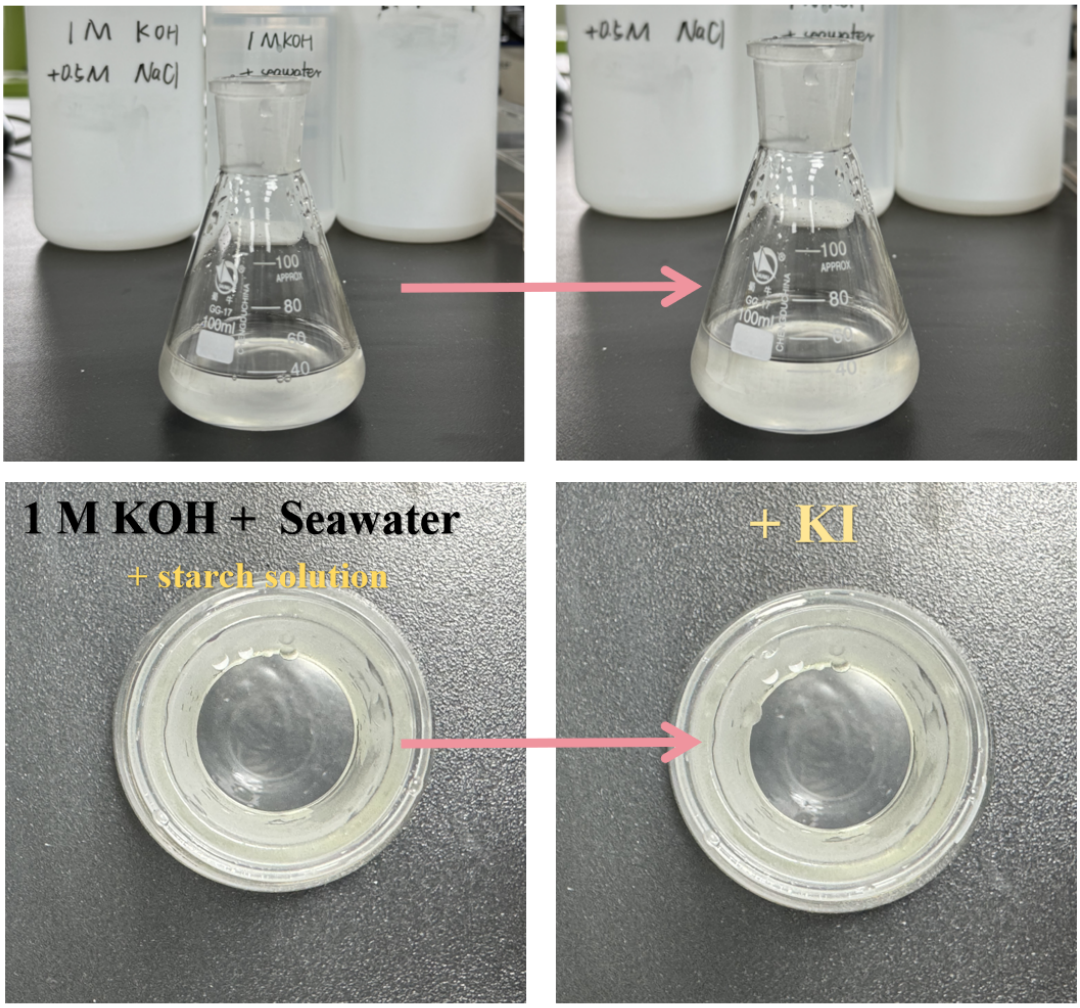

Fig. S31 Digital photos of illustrating the determination of ClO^- in natural seawater.

Fig. S32 Schematic diagram of illustrating the determination of ClO^-.

References

1 W. Zhao, N. Wu, F. Yu, B. Zhou, X. Chu, Z. Wei and S. Yang, *ACS Appl. Energy Mater.*, 2021, **4**, 10976–10985.

2 T. Liang, S. Lenus, Y. Liu, Y. Chen, T. Sakthivel, F. Chen, F. Ma and Z. Dai, *Energy Environ Mater*, 2023, **6**, e12332.

3 S. Zhu, J. Lei, S. Wu, L. Liu, T. Chen, Y. Yuan and C. Ding, *Mater Lett*, 2022, **311**, 131549.

4 E. Saha, K. Karthick, S. Kundu and J. Mitra, *J. Mater. Chem. A*, 2021, **9**, 26800–26809.

5 Y. Dong, Z. Fang, W. Yang, B. Tang and Q. Liu, *ACS Appl. Mater. Interfaces*, 2022, **14**, 10277–10287.

6 W.-H. Huang, X.-M. Li, X.-F. Yang, H.-B. Zhang, F. Wang and J. Zhang, *Chem. Commun.*, 2021, **57**, 4847–4850.

7 X. Ren, Y. Tian, F. Shaik, J. Yang, R. Liu, K. Guo and B. Jiang, *Adv Sustainable Syst*, 2022, **6**, 2100436.

8 J. Wang, D. T. Tran, K. Chang, S. Prabhakaran, D. H. Kim, N. H. Kim and J. H. Lee, *ACS Appl. Mater. Interfaces*, 2021, **13**, 42944–42956.

9 D. Chinnadurai, S. J. Lee, Y. Yu, S. Y. Nam and M. Y. Choi, *Fuel*, 2022, **320**, 123915.

10 S.-C. Lim, C.-L. Chiang, C.-K. Peng, W.-B. Wu, Y.-C. Lin, Y.-R. Lin, C.-L. Chen and Y.-G. Lin, *Chem Eng J*, 2023, **452**, 139715.

11 H. Li, H. Fu, J. Yu, L. Wang, Y. Shi and L. Chen, *J Alloys Compd*, 2022, **922**, 166254.

12 P. Asen, A. Esfandiar and A. Iraji Zad, *Int J Hydrogen Energy*, 2022, **47**, 32516–32530.

13 T. L. L. Doan, D. T. Tran, D. C. Nguyen, D. H. Kim, N. H. Kim and J. H. Lee, *Adv Funct Mater*, 2021, **31**, 2007822.